

RESEARCH ARTICLE

Molecular characterization of a Novel NAD⁺-dependent farnesol dehydrogenase *SoFLDH* gene involved in sesquiterpenoid syntheses from *Salvia officinalis*

Mohammed Ali¹ , Elsayed Nishawy¹ , Walaa A. Ramadan², Mohamed Ewas¹, Mokhtar Said Rizk¹, Ahmed G. M. Sief-Eldein¹, Mohamed Abd S. El-Zayat¹, Ahmed H. M. Hassan¹, Mingquan Guo^{3,4}, Guang-Wan Hu^{3,4}, Shengwei Wang⁵, Fatma A. Ahmed⁶, Mohamed Hamdy Amar^{1*} , Qing-Feng Wang^{4,5}

1 Department of Genetic Resources, Desert Research Center, Cairo, Egypt, **2** Genetics and Cytology Department, Biotechnology Research Institute, National Research Centre, Giza, Egypt, **3** Key Laboratory of Plant Germplasm Enhancement and Specialty Agriculture, Wuhan Botanical Garden, Chinese Academy of Sciences, Wuhan, China, **4** Sino-Africa Joint Research Center, Chinese Academy of Sciences, Wuhan, China, **5** Hubei Minzu University, Enshi, China, **6** Department of Medicinal and Aromatic Plants, Desert Research Center, Cairo, Egypt

 These authors contributed equally to this work.

* mohamed.amar@wbrcas.cn



OPEN ACCESS

Citation: Ali M, Nishawy E, Ramadan WA, Ewas M, Rizk MS, Sief-Eldein AGM, et al. (2022) Molecular characterization of a Novel NAD⁺-dependent farnesol dehydrogenase *SoFLDH* gene involved in sesquiterpenoid syntheses from *Salvia officinalis*. PLoS ONE 17(6): e0269045. <https://doi.org/10.1371/journal.pone.0269045>

Editor: Jen-Tsung Chen, National University of Kaohsiung, TAIWAN

Received: January 14, 2022

Accepted: May 12, 2022

Published: June 3, 2022

Peer Review History: PLOS recognizes the benefits of transparency in the peer review process; therefore, we enable the publication of all of the content of peer review and author responses alongside final, published articles. The editorial history of this article is available here: <https://doi.org/10.1371/journal.pone.0269045>

Copyright: © 2022 Ali et al. This is an open access article distributed under the terms of the [Creative Commons Attribution License](https://creativecommons.org/licenses/by/4.0/), which permits unrestricted use, distribution, and reproduction in any medium, provided the original author and source are credited.

Data Availability Statement: All relevant data are within the manuscript and its [Supporting information](#) files.

Abstract

Salvia officinalis is one of the most important medicinal and aromatic plants in terms of nutritional and medicinal value because it contains a variety of vital active ingredients. Terpenoid compounds, particularly monoterpenes (C₁₀) and sesquiterpenes, are the most important and abundant among these active substances (C₁₅). Terpenes play a variety of roles and have beneficial biological properties in plants. With these considerations, the current study sought to clone the NAD⁺-dependent farnesol dehydrogenase (*SoFLDH*, EC: 1.1.1.354) gene from *S. officinalis*. Functional analysis revealed that, *SoFLDH* has an open reading frame of 2,580 base pairs that encodes 860 amino acids. *SoFLDH* has two conserved domains and four types of highly conserved motifs: YxxxK, RXR, RR (X₈) W, TGxxGhaG. However, *SoFLDH* was cloned from *Salvia officinalis* leaves and functionally overexpressed in *Arabidopsis thaliana* to investigate its role in sesquiterpenoid syntheses. In comparison to the transgenic plants, the wild-type plants showed a slight delay in growth and flowering formation. To this end, a gas chromatography-mass spectrometry analysis revealed that *SoFLDH* transgenic plants were responsible for numerous forms of terpene synthesis, particularly sesquiterpene. These results provide a base for further investigation on *SoFLDH* gene role and elucidating the regulatory mechanisms for sesquiterpene synthesis in *S. officinalis*. And our study paves the way for the future metabolic engineering of the biosynthesis of useful terpene compounds in *S. officinalis*.

Funding: This study was funded by the National Natural Science Foundation of China and with Academy of Scientific Research and Technology (ASRT) under the collaboration project between Wuhan Botanical Garden, Chinese Academy of Sciences, Wuhan, 430074, China, and Desert Research Center (DRC), Cairo, Egypt.

Competing interests: The authors have declared that no competing interests exist.

Abbreviations: EOs, Essential oils; OE, Overexpression; Semi-RT-PCR, Semiquantitative RT-PCR; *SoFLDH*, *S. officinalis* NAD⁺-dependent farnesol dehydrogenase; TPS, Terpene synthase.

Background

The genus *Salvia* (Lamiaceae) includes more than (>1,000) species of woody aromatic shrubs, among which e.g., *S. epidermidis*, *S. japonica*, *S. fruticosa*, *S. tuxtlensis*, *S. miltiorrhiza*, *S. aureus*, *S. przewalskii*, *S. hydrangea*, *S. isensis*, *S. tomentosa*, *S. santolinifolia*, *S. lavandulifolia*, *S. chloroleuca*, *S. glabrescens*, *S. nipponica*, *S. macrochlamys*, *S. allagospadonopsis* and *S. recognita* are economically important and cultivated worldwide for its medical properties and their output of essential oils (EOs). Most of *Salvia* plant species are commonly spread universally in three areas but largely grown in South and Central America (~500 species), East and West Asia (~100 and ~200 species) respectively [1–4]. Lately, *Salvia* species EOs have a valued source for aromatic and medical research for discovering and identifying the ingredient-compounds [3–5]. Essential oils of *Salvia* species have antimicrobial, anticancer, anti-inflammatory, antioxidant, choleric and antimutagenic properties [6–8].

It is well-known that Terpenoid form is the major cluster of natural compounds and a set of secondary metabolites, that have been identified from plant kingdom and other organisms with more than (>40,000) different structures [9]. Terpenoid derives its structural from the isopentenyl diphosphate (IPP), which involves five carbon atoms (C5) [10, 11]. However, the origin name of these different structures arises from the terebinth tree (*Pistacia terebinthus*), all of these identified as different structures terpene. The structure of the terpene unit was illustrated by Wallach and Altered by Ruzicka [12–15]. Some terpenes are related to the plant primary metabolism such as the carotenoid pigments, phytol side chain of chlorophyll, gibberellin plant hormones, and phytosterols of cellular membranes [16, 17], which are important for development and flower blooming of the plants. However, wide ranges of terpenes have been identified as categories of secondary metabolites with essential properties in the adaptation of plants to the stresses. Nonvolatile and volatile terpenes have an important role in the predators of herbivores and defense against photo-oxidative stress, haul of both pollinators and the direct defense against insects and microbes [18]. At present, several studies are focused to understand in-depth the mechanisms of terpene and its functions [3, 4].

It is prominent that *Salvia* species involved high proportion of the essential oil; this fragrant oil mainly contains monoterpenes and sesquiterpenes. The composition of the monoterpenes and sesquiterpenes are differ depends on the plant species and cultivars, in addition to the type of tissues [3, 4, 19–24]. Biosynthesis gene for the sesquiterpene has remained elusive until recently.

The main sesquiterpene in the Egyptian cultivar of *S. officinalis* are Isocaryophyllene, α -caryophyllene, Caryophyllene oxide and (–)-Germacrene D, which are encoded by three unigenes families [3]. So far, their biological or physiological functions have been widely unclear. This makes the enzymes that stimulate the formation both interesting and functionally difficult to differentiate.

Through this research, we focus to clone and functionally expressed the *S. officinalis* NAD⁺-dependent farnesol dehydrogenase (*SoFLDH*, EC: 1.1.1.354) gene in *Arabidopsis thaliana*. The recombinant *SoFLDH* catalyzed the conversion of Farnesyl pyrophosphate (FPP) to the sole produce various types of terpene especially sesquiterpene. *SoFLDH* protein displayed a distinctive amino acid sequence, with highly preserved motifs, including the YxxxK, RXR, RR (X 8) W and TGxxGhaG motifs. Finally, this study reveals to use the protein modeling database to investigate the performance of the 3D structure protein and its function predict.

Materials and methods

Plant materials and tissue collection

Salvia officinalis seeds were kindly provided by the staff member of Egyptian Desert Gene Bank (EDGB) of Desert Research Center (DRC), Egypt. *S. officinalis* seeds had been growing in our growth chamber at National Research Centre (Cairo, Egypt), at temperature of 22°C day/20°C night with humidity of 50–70%, and photoperiod at 16 h day/8 h night, with a light density of 100–150 $\mu\text{moles m}^{-2} \text{s}^{-1}$ using fluorescent bulbs. For gene amplification, young leaves were picked up and instantly cast in liquid nitrogen and stowed at -80°C until RNA extraction.

In silico analysis of *SoFLDH*

SoFLDH nucleotide sequence was carefully selected from our previous RNA-Seq data [3]. The physiochemical assets of the *SoFLDH* were gritty using PROTPARAM website (<http://web.expasy.org/protparam/>). Putative tissue expression profile and cell subcellular localizations for *SoFLDH* gene was built using ePlant and cell eFP (<http://bar.utoronto.ca/eplant/> & http://bar.utoronto.ca/cell_efp/cgi-bin/cell_efp.cgi) based on *Arabidopsis* gene expression and protein localization at different tissues and cell organs. The open reading frames (ORF) for *SoFLDH* was analyzed for the presence of possible transit peptide using bioinformatics tools, iPSORT Prediction (<http://ipsort.hgc.jp/>). Sequence analysis of *SoFLDH* was executed using NCBI BLAST in contradiction of the protein database (<https://blast.ncbi.nlm.nih.gov/Blast.cgi>). Clustal Omega software was used with the default parameters (<https://www.ebi.ac.uk/Tools/msa/clustalo/>) for multiple sequence alignment. Three-dimensional (3D) structure for *SoFLDH* protein was built using SWISS-MODEL (<https://swissmodel.expasy.org>) website based on the closest homologous structures. A maximum likelihood tree was constructed for *SoFLDH* gene using MEGA 6.6 program with default parameters. To assess the phylogeny of the *SoFLDH* protein sequence in relation to other orthologous terpene alcohol dehydrogenases and benzyl alcohol dehydrogenases genes, the protein sequences of characterized terpene alcohol dehydrogenases and benzyl alcohol dehydrogenases were regained from the National Center for Biotechnology Information (NCBI) database, and we looked for the other reported full-length sequences of terpene alcohol dehydrogenases and benzyl alcohol dehydrogenases from *Salvia splendens* (farnesol dehydrogenase; TEY48599.1), *Persicaria minor* (nerol dehydrogenase; AFQ59973.1), *Salvia splendens* (hypothetical protein Saspl_009804; TEY79171.1), *Carpoglyphus lactis* (geraniol dehydrogenase; BAG32342.1), *Castellaniella defragrans* (geraniol dehydrogenase; CCF55024.1), *Arabidopsis thaliana* (Rossmann-fold NAD(P)-binding domain-containing protein; AEE86213.1), *Ocimum basilicum* (geraniol dehydrogenase; AAX83107.1), *Aedes aegypti* (NADP+-dependent farnesol dehydrogenase; ADB03640.1), *Fragaria x ananassa* (cinnamyl alcohol dehydrogenase; AAD10327.1), *Artemisia annua* (cinnamyl alcohol dehydrogenase; ACB54931.1), *Mentha x piperita* ((-)-isopiperitenol dehydrogenase; AAU20370.1), *Lavandula x intermedia* (borneol dehydrogenase; AFV30207.1), *Pseudomonas putida* (p-cumic alcohol dehydrogenase; AAB62297.1), *Nicotiana tabacum* (allyl alcohol dehydrogenase; BAA89423.1), *Arabidopsis thaliana* (allyl alcohol dehydrogenase; AAG50689.1), *Pseudomonas putida* (aryl alcohol dehydrogenase; P39849.1), *Picea abies* (cinnamyl alcohol dehydrogenase; CAA0597.1), *Streptomyces* sp. NL15-2K (coniferyl alcohol dehydrogenase; BAN09098.1), and *Pseudomonas putida* (benzyl alcohol dehydrogenase; AAC32671.1) [25].

RNA extraction and cDNA library preparation

Young leaves of *S. officinalis* were used to extract the total RNA using TransZol Reagent (Focus Bioscience, Australia) according to the manufacturer's instructions and cured with DNase I (Takara). RNA quality was performed on 1.4% Agarose gel, and the clarity was analyzed using a Nanodrop ND1000 (NanoDrop technologies, Wilmington, DE, USA). RNA pools were primed for cDNA libraries using mixing equal volumes from the three RNAs replications in one tube. Two micrograms of total RNA (800 ng approximately) per sample was used for the synthesis of total cDNA with TransScript[®] First-Strand cDNA Synthesis Super-Mix (TransGen Biotech, Beijing, China) according to the manufacturer's instructions. Afterwards, PCR was performed for cDNA synthesis at 42°C for 15 min followed by 85°C for 5 min [3, 4].

QRT-PCR, semiquantitative RT-PCR analysis and Western Blot (WB)

Quantitative RT-PCR was performed by an IQTM5 Multicolor Real-Time PCR Detection System (Bio-Rad, USA) as described previously Ali et al., and Hussain et al., [3, 4, 26, 27] with SYBR Green Master (ROX) (Newbio Industry, China) following the manufacturer's instructions at a total reaction volume of 20 µl. A gene-specific primer for *SoACTIN* forward 5'-GGCAGTTCTCTCCCTCTAT-3' and reverse 5'-GAGGTGGTCGGTGAGAT-3' was used as a reference gene with 157 bp, and *SoFLDH* forward 5'-TTCCTGATCCCTCCAGATT-3' and reverse 5'-CAATGTAGCCATCCGTTGA-3' with 153 bp length. Moreover, semiquantitative real-time PCR was achieved on a Biometra PCR (Biometra T Gradient Thermo block PCR Thermocycler, American Laboratory Trading, San Diego, CA) system with a total reaction volume of 25 µl. A gene-specific primer for *At-B-actin* forward 5'-GGCTGAGGCTGATGATATTC-3' and reverse 5'-CCTTCTGGTTCATCCCAAC-3' was used as a reference gene with 155 bp and the same forward and reverse primers for *SoFLDH*, all the primers were designed using the primer designing tools of IDTdna (<http://www.idtdna.com/scitools/Applications/RealTimePCR/>). The semiquantitative RT-PCR conditions were as follows: pre-denaturation step at 95°C for 4 min, 35 cycles of amplification (95°C for 30 s, 58°C for 30 s and 72°C for 1 min), and a final extension step at 72°C for 10 min. The PCR products were resolved on 1.3% agarose gel, and the expression levels of *At-B-actin* and *SoFLDH* genes were detected. On the other hand, for confirmed the transformation stability of *SoFLDH* protein was isolated and detected from various lines of transgenic and wild-type *A. thaliana* using Western blotting (WB), fresh leaves were homogenized with pestles in prechilled mortars on ice in 1 ml of cold homogenization buffer (100 mM Tris, pH 7.5, 10% sucrose, 5 mM sodium EDTA, and 5 mM sodium EGTA) for each one gram of tissue as described by Ma et al., [28].

Full-length terpene synthase cDNA clone and vector

Full-length cDNAs sequence for *SoFLDH* was obtained based on RNA-Seq sequence information from our transcriptome sequencing of *S. officinalis* plant leaves [3], and *SoFLDH* was amplified from cDNA of young leaf using short and long gene-specific gene primers based on the Gateway pDONR221 vector manual system. The initial PCR amplification was performed by short primers, of *SoFLDH* forward 5'-ATGTGGGGATTAGGTGGGAGT-3' and reverse 5'-TCAATCATGTCACTCACTCACTCAA-3' using the KOD-Plus-Neo DNA polymerase (Novagen) under the following PCR conditions: 3 min at 96°C followed by 10 s at 98°C; 30 s at 60°C (Annealing temperatures), 1.5 min at 68°C, and then 10 min at 68°C. This process was repeated for 33 cycles. The first PCR products was used as a template for the second PCR using long primers, *SoFLDH* forward 5'-GGGGACAAG TTTGTACAAAAAAGCAGGCTTCATGTGG GGATTAGGTGGG-3' and reverse 5'-GGGGACCACTTTG TACAAGAAAGCT GGGTTCAAT

CATGTCACTCACT-3'. BP Clonase (Invitrogen, USA) was used to insert the PCR products into the Gateway entry vector pDONR221. The positive pDONR221-*SoFLDH* constructs harbouring target genes were sequenced and ligated with the destination vector pB2GW7 using Gateway LR Clonase (Invitrogen, USA), then the positive pB2GW7-*SoFLDH* was used for *A. thaliana* plant transformation [3, 4].

***Arabidopsis* plant growth conditions and preparation of *Agrobacterium* cultures for floral-dip transformation**

The ecotype of *A. thaliana* seeds Columbia-0 (Col-0) has prepared for germination by adding 1.2 ml sterilized -water for seeds at a 2.0 ml Eppendorf tube, then nursed at ~4°C for three days at the refrigerator. Then *A. thaliana* seeds had been growing in a growth chamber with humidity of 60–70% under the day and night temperature of 22°C day/20°C night, using a light density of 100–150 mol m⁻² s⁻¹ using fluorescent bulbs and photoperiod at 16 h day/8 h night. For floral-dip transformation, plants at two-month age were used, and one week after, the primary inflorescences were clipped. The Plant watering was stopped at four days before the transformation to increase and improve the transformation efficiency. In addition, the constructs of pB2GW7-*SoFLDH* were introduced into *Agrobacterium tumefaciens* strain GV101 by direct electroporation. Recombinant GV101 was grown for 48 h at 28°C in solid LB media supplemented with 60 µg/ml of each rifampicin and spectinomycin. An individual colony was injected into 0.8 ml of liquid medium and grown at 28°C under 180 rpm agitation overnight with the same media composition. After 24 h, 0.8 ml of each sample of liquid medium was relocated to a 300 ml conical flask containing 60 ml of LB media supplemented with the same compositions; the samples were grown at 28°C in a shaker overnight until an optical density of 0.75 (OD₆₀₀) was reached. Overnight cell cultures were harvested by centrifugation at 4,000 rpm for 12 min at 4°C, and the pellet was resuspended in the floral-dip inoculation medium contained 5.2% sucrose and 0.055% Silwet. *A. thaliana* was transformed by drenched the secondary inflorescences in the inoculation medium and stirred softly to allow the intake of *Agrobacterium* harbouring the pB2GW7-*SoFLDH* vector into the flower gynoecium. The transformed plants were kept in the dark and covered by plastic cover overnight to maintain humidity. After 24 h, the plants were returned back to their normal growth conditions. The transformation was repeated after 7–10 days to increase the transformation efficiency. Plants were grown for additional 30–37 days, until all of the siliques became brown and dry. The seeds were harvested and stored at ~4°C under desiccation [3, 4, 29, 30]. BASTA was used for selection of transformant seedlings which were also confirmed with PCR for positive transgenic lines, more than 12 positive plant lines with selective gene were analysed for terpenoid profiling and target gene expression.

Phenotypic evaluation

Transgenic plants were watered and fertilized regularly with Miracle Gro fertilizer (Scott's Company, USA) prepared according to manufacturer's instructions for phenotypic comparisons between *A. thaliana* transgenic lines and their counterpart wild-type plants. Plants were grown in the growth chamber under the previously reported conditions for vegetative growth and flowering. Plants were assessed with regard to leaf morphology, flowering time, and terpenoid metabolic [4].

Metabolite extraction from transgenic *A. thaliana* leaves

Terpenoid compounds from overexpression of *SoFLDH*-*A.thaliana* and wild type were extracted and isolated. Thirty six leaves from transgenic *A. thaliana* line (three leaf from each

plant) were grind in liquid nitrogen with a mortar and pestle to fine powder, and directly soaked in n-hexane as a solvent in Amber storage bottles, 30 ml screw-top vials with silicone/PTFE septum lids (<http://www.sigmaaldrich.com>) were applied to diminish the loss of volatiles to the headspace then incubated with shaking at 37°C and 200 rpm for 72 h. Afterward, the solvent was transmitted using a glass pipette to a 10 ml glass centrifuge tube with screw-top vials with silicone/PTFE septum lids and centrifuged at 5,000 rpm for 10 min at 4°C to remove plant debris. The supernatant was pipette into glass vials with a screw cap and oil was concentrated until remaining 1.5 ml of concentrated oils under a stream of nitrogen gas with a nitrogen evaporator (Organomation) and water bath at room temperature (Toption-China-WD-12). The concentrated oils transferred to a fresh crimp vial amber glass, 1.5 ml screw-top vials with silicone/PTFE septum lids were used to diminish the loss of volatiles to the headspace. For absolute oil recovery, the remaining film crude oil in the internal surface of concentrated glass vials was dissolved in the minimum volume of n-hexane, thoroughly mixed and transferred to the same fresh crimp vial amber glass, 1.5 ml. And the crimp vial was placed on the auto sampler of the gas chromatography mass spectrometer (GC-MS) system for GC-MS analysis, or each tube was covered with parafilm after closed with screw-top vials with silicone/PTFE septum lids and stored at -20°C until GC-MS analysis [3, 4, 31].

GC-MS analysis of essential oil components

GC analysis was implemented using a Shimadzu model GCMS-QP2010 Ultra (Tokyo, Japan) system. 1 µl aliquot of each sample was introduced (split ratios of 15:1) into a GC-MS equipped with an HP-5 fused silica capillary column (30 m x 0.25 mm ID, 0.25 µm film thicknesses). Helium was used as the carrier gas at a constant flow of 1.0 ml/min⁻¹. The mass spectra were monitored between 50–450 m/z. Temperature was initially under isothermal conditions at 60°C for 10 minutes. Temperature was then increased at a rate of 4°C/min⁻¹ to 220°C, held isothermal at 220°C for 10 minutes, increased by 1°C/min⁻¹ to 240°C, held isothermal at 240°C for 2 min, and finally held isothermal for 10 minutes at 350°C. The identification of the volatile constituents was determined by parallel comparison of their recorded mass spectra with the data stored in the Wiley GC/MS Library (10th Edition) (Wiley, New York, NY, USA), the Volatile Organic Compounds (VOC) Analysis S/W software, and the NIST Library (2014 edition). The relative percent amount of each component was calculated by comparing its average peak area to the total areas. All of the experiments were performed simultaneously three times under the same conditions for each isolation technique with total GC running time was 80 minutes [3, 4, 31].

Results and discussion

In silico analysis of *SoFLDH*

The *SoFLDH* gene with 2,580 bp of open reading frame, which encodes a 860 amino acid and a 95.114 kDa of molecular mass and a 8.59 PI of theoretical isoelectric point (pI). The surmised amino acid sequence of *SoFLDH* showed signal peptide longer than monoterpene synthases (600–650 aa), and other sesquiterpene synthases of 550–580 aa. Furthermore, the presence of 30 amino acid long targets sequence using ‘iPSORT’ program suggested that *SoFLDH* protein was localized into the Mitochondrial and chloroplast where sesquiterpene and triterpene biosynthesis takes place. BLASTX analysis revealed that the *Salvia splendens* farnesol dehydrogenase was the nearest homologue gene to *SoFLDH*, with 91.74% identity, 91% Query cover and 0.0 E-value (<https://blast.ncbi.nlm.nih.gov/Blast.cgi>). Also, from the phylogenetic tree analysis we found the surmised amino acid sequence of *SoFLDH* similar to farnesol dehydrogenase (TEY48599.1) gene from *Salvia splendens*, and other terpene alcohol dehydrogenases and

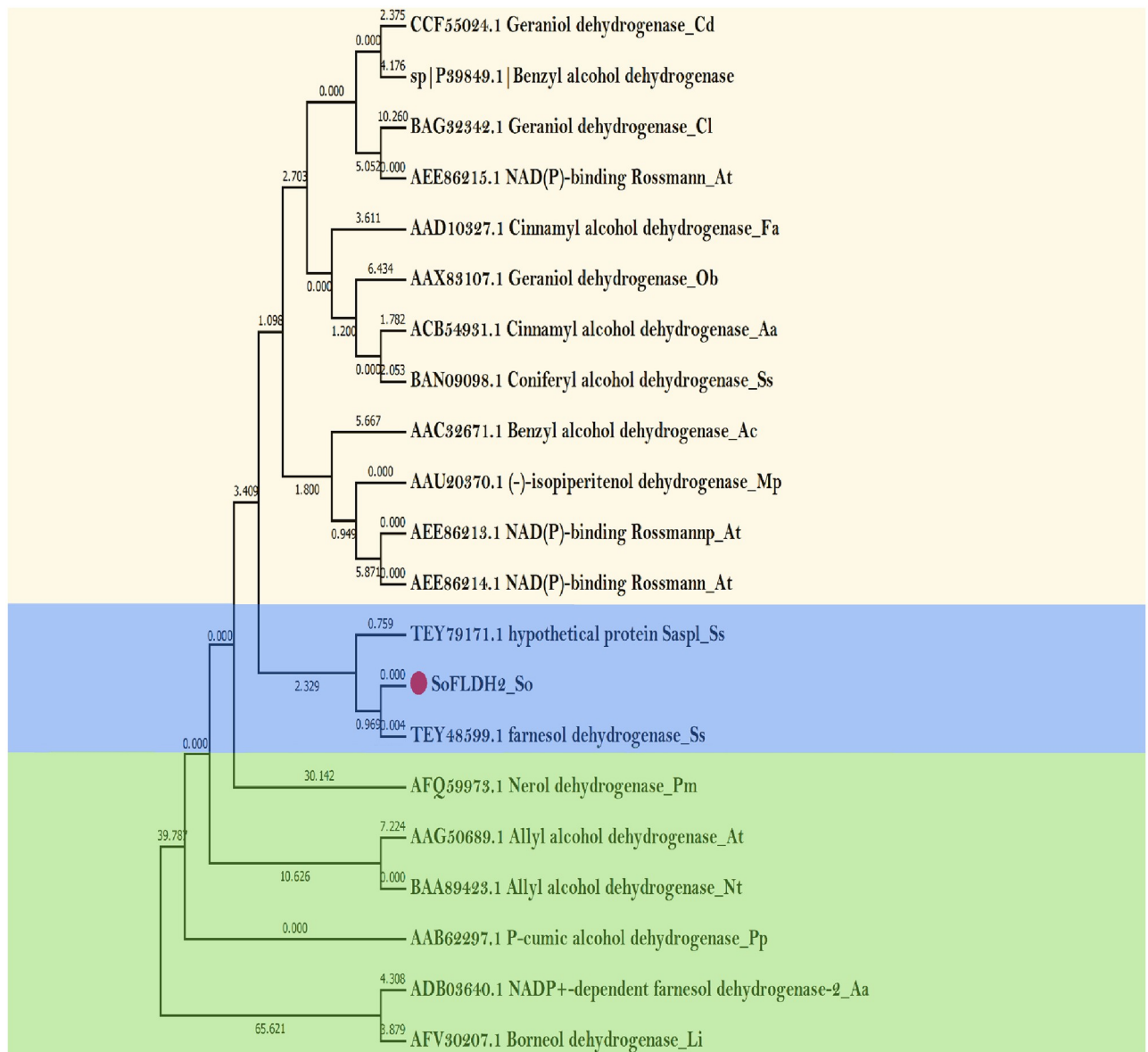


Fig 1. Phylogenetic analysis of *SoFLDH* gene from *S. officinalis* and other plants, based on the primary amino acid sequences. A maximum likelihood tree was constructed for *SoFLDH* gene using MEGA 6.6 program with default parameters. The percentage of bootstrap values is provided in the branches. Sequences are labeled with the accession numbers and species names.

<https://doi.org/10.1371/journal.pone.0269045.g001>

benzyl alcohol dehydrogenases genes from different plant species (Fig 1). The function of *SoFLDH* gene was initially foretold depended on sequence alignment with well-known others terpene alcohol dehydrogenases and benzyl alcohol dehydrogenases genes sequences and other conserved motifs from Lamiaceae family and other plants (Fig 2). For instance, *SoFLDH* protein contained two highly conserved motifs YxxxK (residues 9–13) and (residues 585–589) motifs. Moreover, *SoFLDH* protein contained other commonly conserved RXR motif (residues 285–287), which is important for product cyclization in Class III TPS proteins [32–34] (Fig 2). Furthermore, *SoFLDH* protein contained another conserved motif such as, RR (X8) W (residues 405–415) region, which are located in most of the sesquiterpene syntheses were

	YxxxK	
AEE86213.1	-----	0
<i>SoFLDH</i>	MWGLGGSH YWGRKES SGKVEGIVVVFAWMSSQEKHLKKNYVDMYSSRGWNSIVCQPQFLNLF	60
TEY48599.1	MWGLGGSH YWGRKES SGKVEGIVVVFAWMSSQEKHLKKNYVDMYSSRGWNSIVCQPQFLNLF	60
TEY79171.1	MWGLGGSH YWGRKER GKVEGIVVVFAWMSSQEKHLKKNYVDMYSSRGWNSIVCQAQFLNLF	60
AEE86213.1	-----	0
<i>SoFLDH</i>	FDPKAASLAQEIVNELIQENLKGIDLDLSENELKIRPCPIIFASFSGGPKACMYKVLQII	120
TEY48599.1	FDPKAASLAQEIVNELIQENLKGIDLDLSENELKIRPCPIIFASFSGGPKACMYKVLQII	120
TEY79171.1	FDPKAASLAQEIVNELIQENLKGIE-----LKIRPCPIIFASFSGGPKACMYKVLQII	113
AEE86213.1	-----	0
<i>SoFLDH</i>	EGKWEEQINQDECRLVRDSISGYIFDSCPVDVSDMGNRFFHHQTGLTISRPLIASWIT	180
TEY48599.1	EGKWEEQINQDECRLVRDSISGYIFDSCPVDVSDMGNRFFHHQTGLTISRPLIASWIT	180
TEY79171.1	EGKCEEQINLDECRLVRDSISGYIFDSCPVDVSDTGNRFFLHQGLTISRPLIASWIT	173
AEE86213.1	-----	0
<i>SoFLDH</i>	SGISSTLDTLFLSRFESQRAEYWQTLYSTVSVFRAPYLILCSEDELAPFQII FNFATRLK	240
TEY48599.1	SGISSTLDTLFLSRFESQRAEYWQTLYSTVSVFRAPYLILCSEDELAPFQII FNFATRLK	240
TEY79171.1	SGISSTLDALFLSRFESQRAEYWQTLYSTVSVFRAPYLILCSEDELAPFQII FNFATRLK	233
	RxR	
AEE86213.1	-----	0
<i>SoFLDH</i>	NLGADVKLKWNKSSHVGHFRHHPEEYSASVTELLTKASITYSQ RIRQ LEGEKMGMEGGH	300
TEY48599.1	NLGADVKLKWNKSSHVGHFRHHPEEYSASVTELLTKASITYSQ RIRQ LEGEKMGMEGGH	300
TEY79171.1	NLGADVKLKWNKSSHVGHFRHHPEEYSAVTELLSKAAITYSQ RIRQ LEGEKMGMEGGH	293
AEE86213.1	-----	0
<i>SoFLDH</i>	DEISYPFNGLRKTATMSRDSLHRVNLNDYFHVPSVVEYHEDRAVGSIPDESKGRYIPL	360
TEY48599.1	DEISYPFNGLRKTATMSRDSLHRVNLNDYFHVPSVVEYHEDRAVGSIPDESKGRYIPL	360
TEY79171.1	DEISYPFNGLRKAAMSRLHRVNLNDYFHVPSVVEYHEDRVDGSI PDESKGRYIPL	353
	RR (X) 8 W	
AEE86213.1	-----	0
<i>SoFLDH</i>	SSPPKISAHGVLGEFLDACVPKNVEDWDLRFSPSMRSAAFASG RRYLNLNPPFWLS AEAA	419
TEY48599.1	SSPPKISAHGVLGEFLDACVPKNVEDWDLRFSPSMRSAAFASG RRYLNLNPPFSL SGSL	420
TEY79171.1	SSPPKISAHGVLGQFLDACVPKNVEDWDLRFSPSMRSAAFASG RRSSPFNPIKWH SGQE	413
	TGxxGhaG	
AEE86213.1	---MGPKMPTETENMKILV TGSTYLG ARLCHVLLRRGHSVRALVVRTS DLSLDPPE-	55
<i>SoFLDH</i>	CL-KVPIITLPLTSRRMLFCV TGASGYLGG RRLCHALLDQGYSVKAFVRKSSDVSSLPPPS	478
TEY48599.1	PLES-SNHTATNQ PARKVALV TGASGYLGG RRLCRALLHQGYSVKAFVRKTS D ISSLPPP-	478
TEY79171.1	YEEM-PDYREFSTRKYLDLSLV TGASGYLGG RRLCHALLHQGYSVKAFVRKTS DVSSLPPS	472
	:*.***. ** *: **: *: **: *: **: *: *	
AEE86213.1	-----VELAYGDVTDYRSLTDACSGCDIVFHAALVEPWLDPDSRFISVNVGGLKNVLE	109
<i>SoFLDH</i>	GDGGGSLQLVYGDVTDYPSLLEAFSGCHVVFTAAALVEPWLDPDSRFISVNVGGLKRVLK	538
TEY48599.1	SAAGGSLQLVYGDVTDYPSLLEAFSGCHVVFTAAALVEPWLDPDSRFITTVNVGGLKRVLK	538
TEY79171.1	DAADGSLQLVYGDVTDYPSLLEAFSGCHFVFTAAALVEPWLDPARFTSVNVGGLKRVLK	532
	*: ***** ** : * ** . *** : ***** : ** : ***** : ** :	
	YxxxK	
AEE86213.1	AVKET---KTVQKIIYTSFFALGSTDGSVANENQVHNERFFCTE YERSK AVADKMALN	165
<i>SoFLDH</i>	AYKETEMETETIEKIIYTSFFALGSTDGYIADETQVHPAKHFCTE YEKSK AISDKIALD	598
TEY48599.1	AYKET---ETIEKIIYTSFFALGSTDGYIADETQVHPAKHFCTE YEKSK AVSDKIALD	594
TEY79171.1	AYTET---ETIEKIIYTSFFALGSTDGYIADETQVHPAKHFCTE YEKSK ALSDKIALD	588
	* ** :*: ***** :*: * ** : ***** :*: ***** :*	

Fig 2. Multiple sequence alignment. The deduced amino acid sequence of *SoFLDH* was aligned with homologues identified from the BLASTX analysis. The conserved motifs YxxxK, RxR, RR(X)8 W and TGxxGhaG are marked. *SoFLDH*: NAD⁺-dependent farnesol dehydrogenase [*Salvia officinalis*]; farnesol dehydrogenase [*Salvia splendens*: TEY48599.1]; hypothetical protein Saspl_009804 [*Salvia splendens*: TEY79171.1]; NAD(P)-binding Rossmann-fold superfamily protein [*Arabidopsis thaliana*, AEE86213.1].

<https://doi.org/10.1371/journal.pone.0269045.g002>

marked in (Fig 2). Also, SoFLDH protein contained another conserved motif TGxxGhaG (residues 440–447), and all these previous motifs have previously stated to flank the entrance of the active site. The nucleotide-binding motif TGxxxGhG is the highly conserved motif for coenzyme binding and the stabilizing the central β -sheet. Moreover, the YxxxK motif displays the catalytic center [35] and remains responsible for the predilection for NADP(H) over NAD(H) [36, 37]. Finally, each protein sequences have one or two or all of these conserved domains are belong to the terpene synthase family [3, 4, 11, 38–40].

Putative tissue expression pattern and subcellular localizations of *SgCINS* gene

We analyzed the putative *SoFLDH* gene expression profile maps based on Arabidopsis transcript expression for further understanding the functions of *SoFLDH* gene at different Arabidopsis tissues (Fig 3a–3c). It is clear from the Arabidopsis Electronic Fluorescent Pictograph Expression Profile Browser that the *SoFLDH* gene was expresses at all Arabidopsis tissues. And *SoFLDH* gene was highly expressed at Root then Petals, Sepals and Hypocotyl (Fig 3a). In context, *GmTPS21*, *SoHUMS*, *SoLINS2*, *SoNEOD*, *SgTPSV*, *SgFARD* and *SgGERIS* genes from *G. max*, *S. officinalis* and *S. guaranitica* were reported with higher expression levels in roots and seeds by liu et al., and Ali et al., [3, 4, 41], respectively. Moreover, the putative tissue specific stem epidermis for *SoFLDH* was analyzed and we found the highly expressed was record in top of stem epidermis more than the bottom of stem epidermis (Fig 3b). Furthermore, the putative subcellular localizations of *SoFLDH* was analyzed based on Arabidopsis protein localization for identified the *SoFLDH* synthesis sites at different cell organs (cell plate, cytoskeleton, cytosol, extracellular, golgi, endoplasmic reticulum, plasma membrane, mitochondrion, nucleus, peroxisome, plastid, unclear, unknown and vacuole) (Fig 3c). It is clear from the Arabidopsis Cell Electronic Fluorescent Pictograph subcellular localizations profiles that the *SoFLDH* gene was highly expressed and presented in plasma membrane then endoplasmic reticulum, vacuole, cytosol, mitochondrion, golgi pody and plastid (Fig 3c). These results are in line with Ali et al., Taniguchi et al., Chen et al., and Wang et al., [26, 42–44] who reported that most of TPSs genes were targeted to the plastid or other cell organelles such as mitochondrion and nucleus.

Tissue-specific expression of *SoFLDH* gene by quantitative RT-PCR

To determinate the organ-specific expression pattern of *SoFLDH*, we quantified the expression levels of *SoFLDH* transcripts in *S. officinalis* young leaves, old leaves, stems, bud flowers, flowers and roots tissues using qPCR-PCR (Fig 4). From our results, we found the *SoFLDH* gene is expressed in all tissue with distinct expression patterns. In old leaves, *SoFLDH* transcripts gene showed the highest expression levels, followed by stems, flowers, bud flowers, young leaves and roots (Fig 4). Similar results were obtained by Ali et al., [4] of which, the highest expression for sesquiterpene gene encoded by Selinene synthase (*SgTPS-3*) was reported in old leaves, followed by bud flowers [4].

The 3D structure of *SoFLDH* protein

SoFLDH protein sequence contains large, conserved domain, which was identified using the InterPro protein sequence analysis & classification (<https://www.ebi.ac.uk/interpro/>) database. In context that, The SoFLDH protein with a 860-aa length has an NAD(P)-binding domain superfamily domain (IPR036291) from 433–625 aa, and this previous domain have overlapping entries with other domains superfamily, such as Oxidoreductase, N-terminal (IPR000683), Semialdehyde dehydrogenase, NAD-binding (IPR000534), Lactate/malate

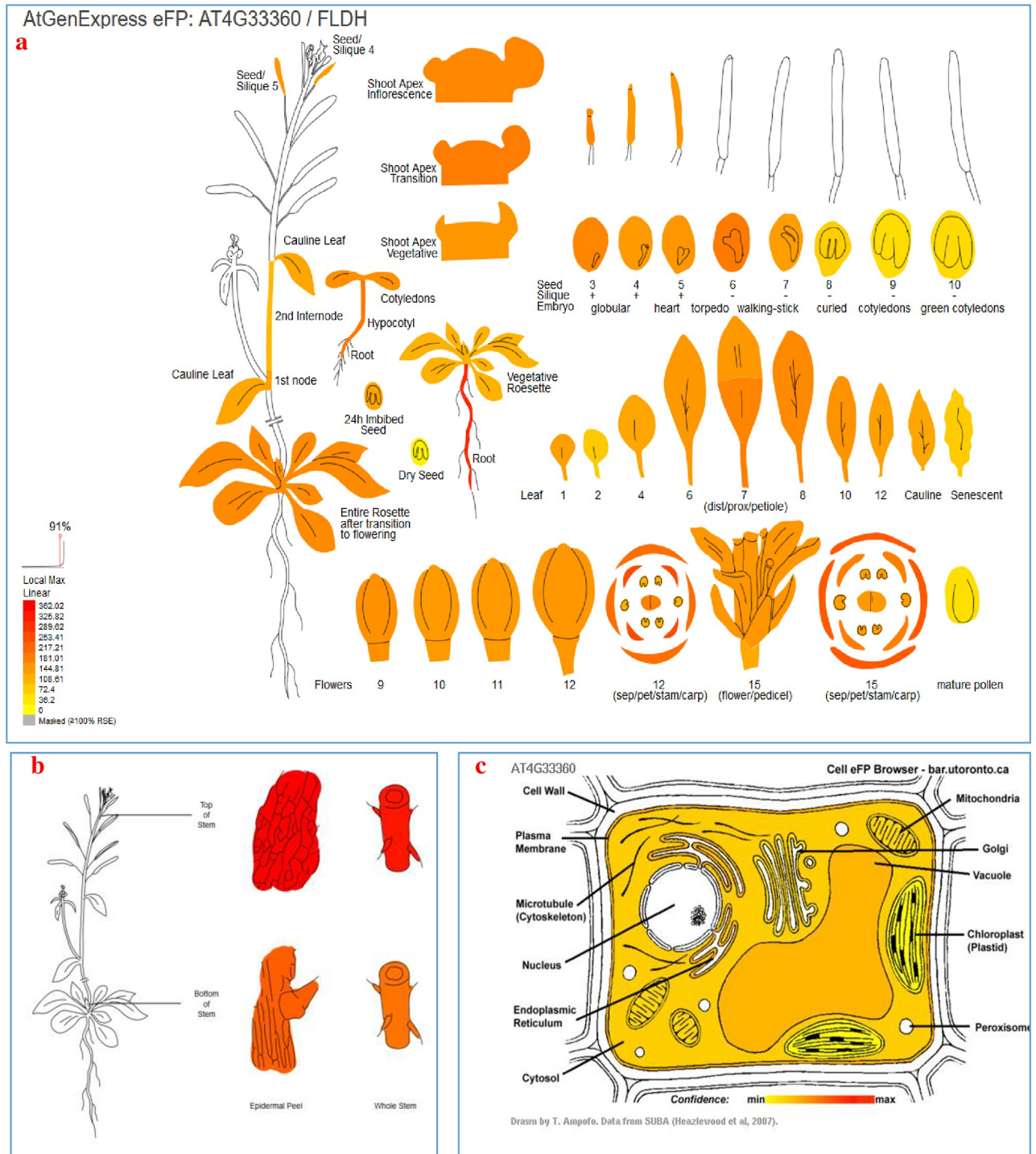


Fig 3. Visualization the putative an “electronic fluorescent pictograph” browsers for exploring the putative tissue expression and cell localization of *SoFLDH* (AT4G33360) gene, based on *Arabidopsis* gene expression and protein localization at different tissues and cell organs. a Expression data at different tissues from seedling to flowering stages. **b** Expression data of tissue specific stem epidermis at top and bottom. **c** Expression data at different cell organs. The blue arrow points the expression scale (the more intense red color, the more gene expression).

<https://doi.org/10.1371/journal.pone.0269045.g003>

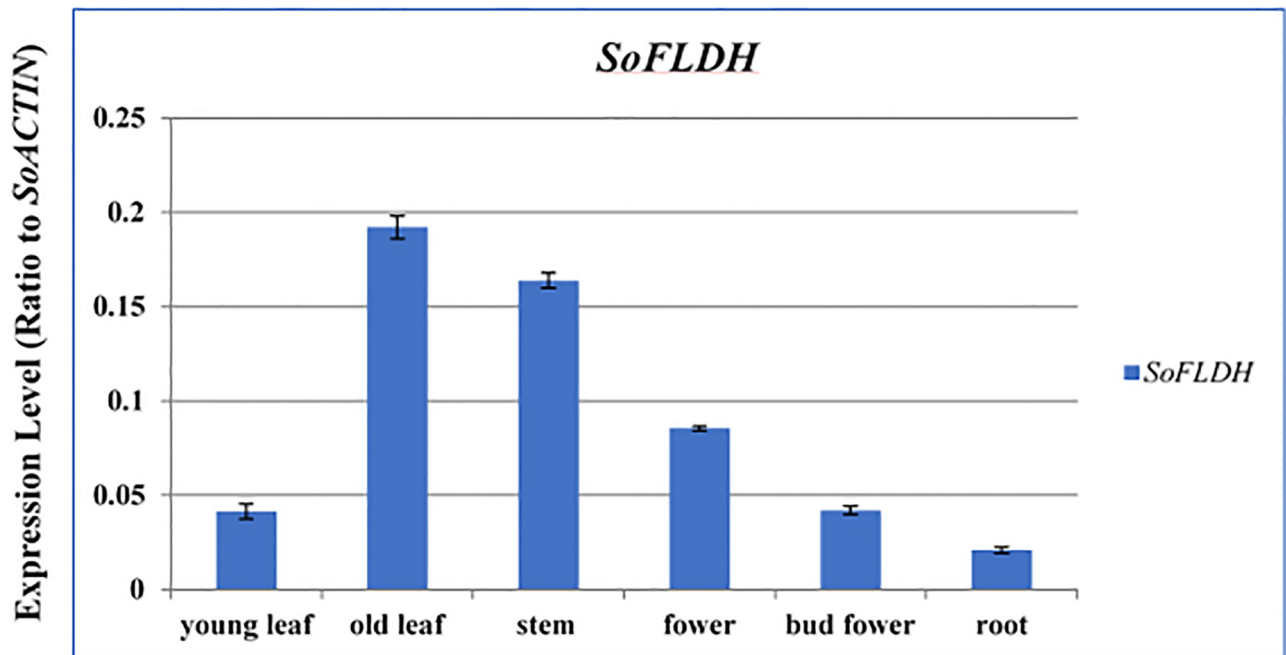


Fig 4. Quantitative RT-PCR validation of expression of *SoFLDH* gene from various tissues of *S. officinalis*. Total RNAs were extracted from young leaves, old leaves, stem, flower, bud flower and root samples and the expression of *SoFLDH* gene was analyzed using quantitative real-time. *SoACTIN* was used as the internal reference. The values are means \pm SE of three biological replicates.

<https://doi.org/10.1371/journal.pone.0269045.g004>

dehydrogenase, N-terminal (IPR001236), Dihydrodipicolinate reductase, N-terminal (IPR000846), and NAD-dependent epimerase/dehydratase (IPR001509). This domain is shown in the 3D model built using SWISS-MODELserver (<https://swissmodel.expasy.org>). The 3D protein model was constructed using UDP-N-acetylglucosamine C4-epimerase (PelX) gene that belong to short-chain dehydrogenase/reductase (SDR) superfamily from *Pseudomonas aeruginosa* [PDB accession: 6wjb] as a template [45] (Fig 5). From the 3D model, *SoFLDH* was shown to consist entirely of alpha-helices and beta-sheets, long and short connecting loops and turns. Four conserved domains NAD 1: Nicotinamide-Adenine-Dinucleotide, NAD 3: Nicotinamide-Adenine-Dinucleotide, UD1.2: Uridine-Diphosphate-N-Acetylglucosamine and UD1.4: Uridine-Diphosphate-N-Acetylglucosamine were found in the ligands pocket, which encompass the active site (Fig 5).

Functional characterization of *SoFLDH* gene in transgenic *A. thaliana* leaves

The function and specificity of *SoFLDH* have been detected by *A. thaliana* Columbia-0 (Col-0) transgenic plants. Overexpression of *SoFLDH* in *A. thaliana* was achieved using *Agrobacterium tumefaciens* strain GV101 harboring the transformation vector pB2GW7-*SoFLDH*. Twelve BASTA-resistant transgenic *A. thaliana* were generated with longer flowering stems (Fig 6a and 6b). In contrast, the transgenic *A. thaliana* showed longer flowering stems with many flowers compare with wild-type (Fig 6a). Expression of the *SoFLDH* gene in positive transgenic *A. thaliana* was confirmed using semi-quantitative RT-PCR (Fig 6b). The transcription level of the transgenic plants were verified using Quantitative RT-PCR (Fig 6c). Leaves of twelve 35-day-old transgenic plants and wild types were sampled for RNA isolation and cDNA synthesis. The transgenic plants represent high expression of the *SoFLDH* gene than wild-type.

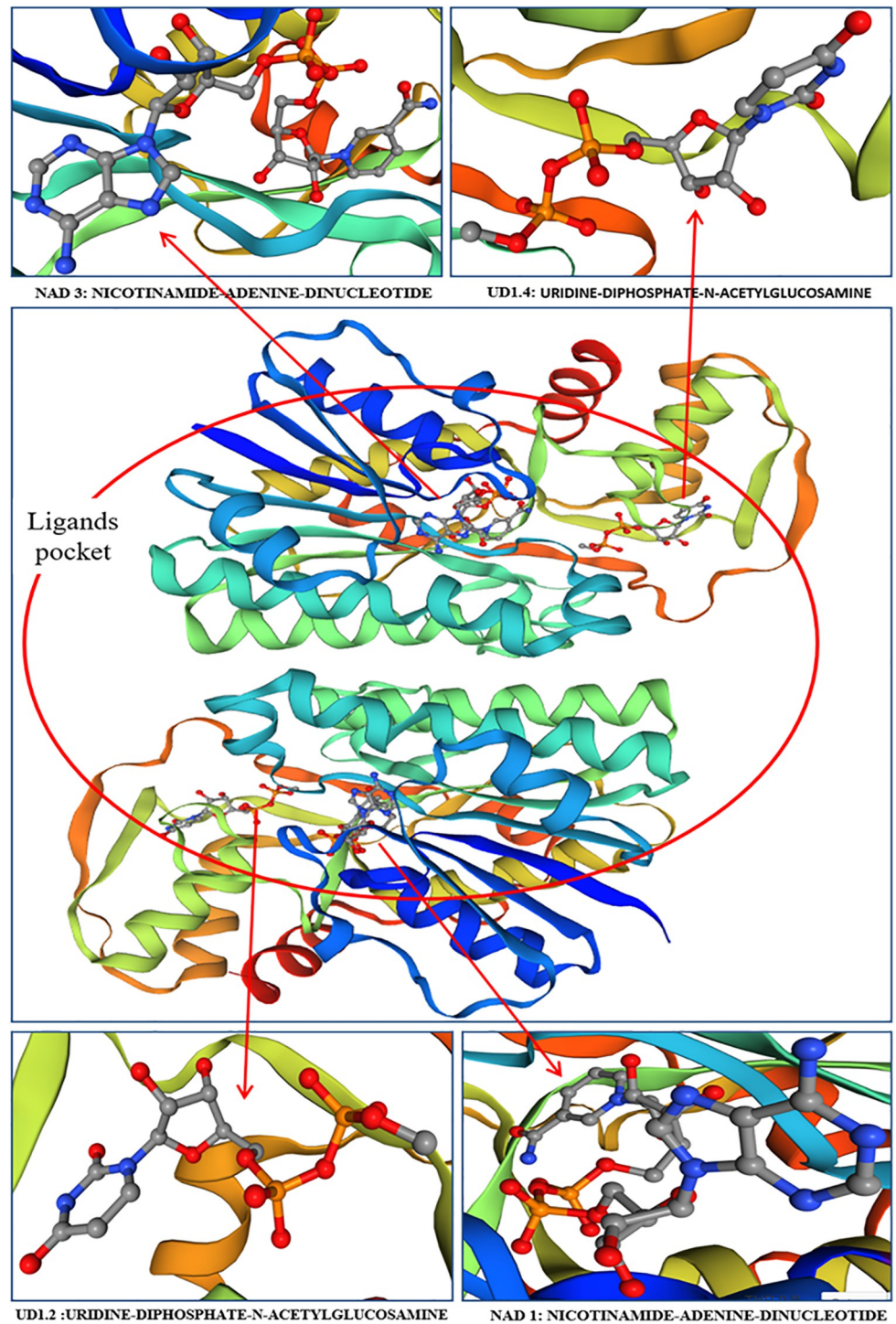


Fig 5. Predicted 3D model of *SoFLDH* generated by the SWISS-MODEL software. The arrows represent the ligands pocket with predicted active binding residues, the Nicotinamide-adenine-dinucleotide (NAD) domain and the Uridine-diphosphate-n-acetylglucosamine (UD) domain.

<https://doi.org/10.1371/journal.pone.0269045.g005>

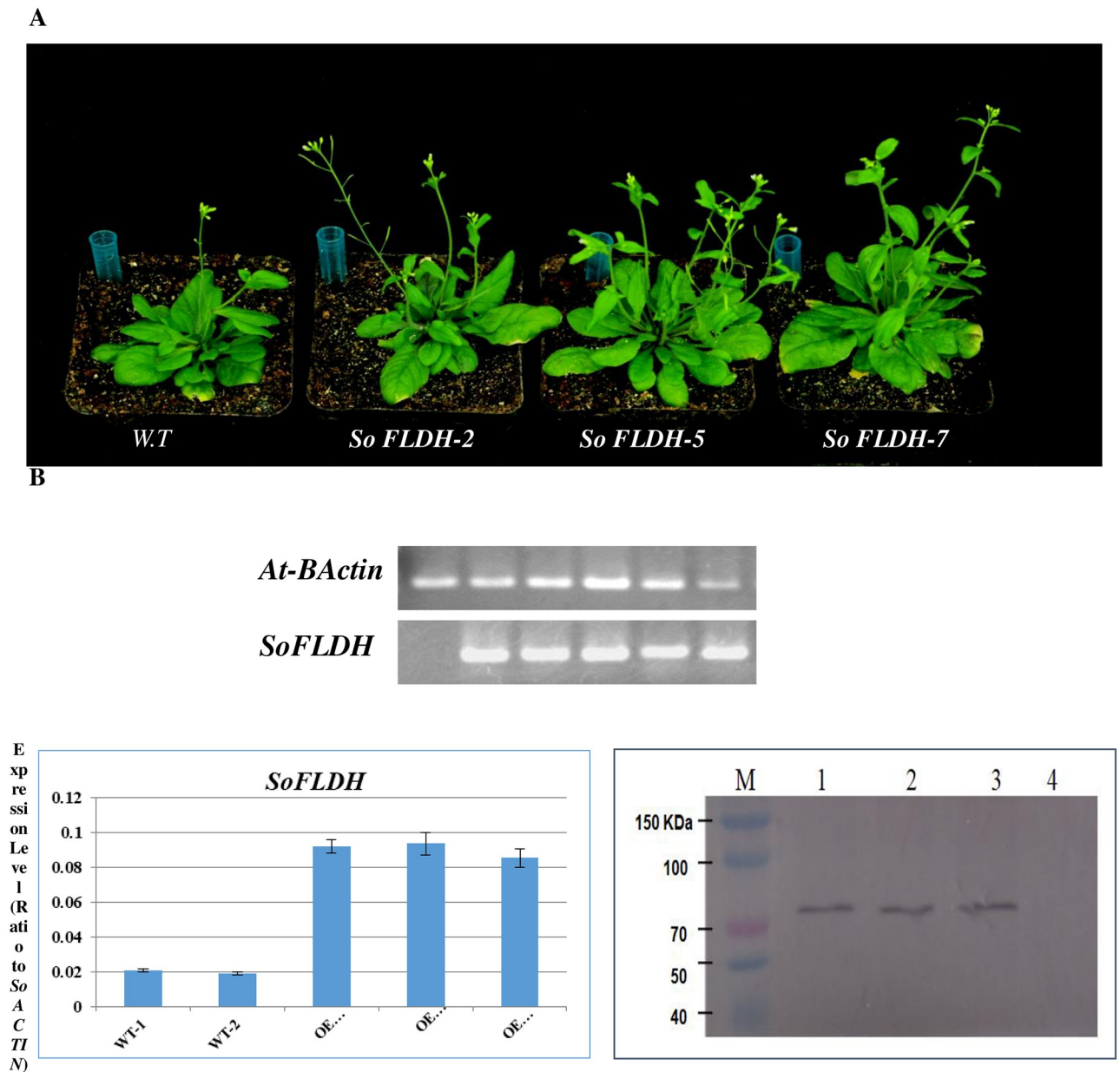


Fig 6. Overexpression of *SoFLDH* gene in transgenic *Arabidopsis*. (A) Comparison of the phenotypes of the transgenic and wild type *A. thaliana*. (B) Semiquantitative RT-PCR to confirm the expression of terpeneoid genes. (C) Quantitative RT-PCR validation of expression of *SoFLDH* gene from wild-type and transgenic *A. thaliana* lines. (D) Western blotting (WB) detection of *SoFLDH* protein in transgenic and wild-type *A. thaliana*, the first left-hand most lane represent molecular marker proteins (M), *OE-SoFLDH-2* (lane 1), *OE-SoFLDH-5* (lane 2), *OE-SoFLDH-7* (lane 3) and wild-type (W.T; lane 4).

<https://doi.org/10.1371/journal.pone.0269045.g006>

Moreover, we used Western blotting (WB) analysis for confirmed the transformation stability by *SoFLDH* gene, and protein expression success (Fig 6d). This finding confirmed that the *SoFLDH* gene was overexpressed successfully in *A. thaliana*. Based on the transcription level and WB analysis results, we select *OE-SoFLDH-2*, *OE-SoFLDH-5* and *OE-SoFLDH-7* for further analysis. Meanwhile the morphological analysis resulted in delayed in flowering formation in wild type compared to the transgenic plants (Fig 6a). In context, this results are in line with Ali et al., [3, 4], which found that the overexpression of terpenoids and TPS synthesis genes,

such as *SoLINS*, *SoNEOD*, *SoTPS6*, *SoSABS*, *SoCINS*, *SgGPS*, *SgFPPS* and *SgLINS* from *S. officinalis* and *Salvia guaranitica* in *Nicotiana tabacum* and *A. thaliana*, occurred delayed in growth and flowering formation in wild type plants compared to the transgenic plants.

Terpene contents in transgenic *A. thaliana* leaves

The metabolite was analyzed by GC-MS to recognize the unique terpenes that formed by transformation with the *SoFLDH* gene (S1 Fig). The mono-, sesqui- and diterpene peaks were obviously measured. The type and number of metabolites were displayed by the percentage of peak area (% peak area) (Table 1). We are using the mass spectra libraries, reported references and the extracts of wild-type *Arabidopsis* which produce disparate amounts and types from terpenoids for identified the terpenes in wild type and transgenic *A. thaliana*. As expected, the leaves of transgenic *A. thaliana* plants emitted a high level of various terpenoids compare with leaves of wild-type. Furthermore, in transgenic *A. thaliana* leaves the diterpene compounds were reported as the main group after (30.49%), followed by sesquiterpenes group (15.46%) then one monoterpene compound (0.89%). While, in wild-type *A. thaliana* the diterpene compounds group was detected as the only group (13.12%) (S1 Fig and Table 1). Moreover, the results shown in S1 Fig and Table 1, represent clear alteration in the transgenic plants, with many new peaks at 29.297, 30.303, 32.328, 35.301, 39.599, 49.213 and 63.242 of retention time. This peak was identified as Levo- β -Elemene, Cis-Caryophyllene, Gamma.-Muuroolene, (-)- β -Bourbonene, Cis-Thujanol, Trans-Phytol and Farnesan, based on the nearest hit from a search of the Wiley GC/MS, NIST Library and VOC Analysis S/W software (S1 Fig and Table 1). The production of various terpene by overexpression of *SoFLDH* gene in *A. thaliana*, was getting previously by [4, 29]. With more direct interest in our results, the *SoFLDH* was responsible for the production of various types of terpene specially sesquiterpene through the same common isoprenoid pathway in sesquiterpene biosynthesis. It is worth noting that our results are in lines with several previously evidence supported that various terpene synthases genes have ability to synthesize a number of metabolite simultaneously, like, carene synthases, (\pm)-linalool synthases, cineole synthases, myrcene synthase, β -amyrin synthases and terpinolene synthases [10, 11, 46–49].

Conclusions

The present study highlighted to clone and functionally identify one of the narrowly expressed sesquiterpene synthase (*SoFLDH*), which is responsible for the production of NAD⁺-dependent farnesol dehydrogenase [EC:1.1.1.354] in *S. officinalis*. Overexpression *SoFLDH* in *A. thaliana* resulted in accelerating the growth and flowering of *OE-SoFLDH-2*, *OE-SoFLDH-5* and *OE-SoFLDH-7* transgenic lines. These three lines exhibited a high expression of the *SoFLDH* gene, which regulate the production of various terpenes. The various types of terpene especially sesquiterpene formed in these *A. thaliana* transgenic plants reveal the dexterity of *A. thaliana* for synthesizing the same product through the common mevalonate pathway of sesquiterpene biosynthesis. While, *SoFLDH* protein exhibits a strong sequence similarity to farnesol dehydrogenase (TEY48599.1) gene from *Salvia splendens*, in addition to other terpene alcohol dehydrogenases and benzyl alcohol dehydrogenases genes from different plant species. Whereas, *SoFLDH* protein contained four types from highly conserved motifs YxxxK, RXR, RR (X8) W, TGxxGhaG and four conserved domains in the ligands pocket, and these previous domains have overlapping entries with another important superfamily domain. Overall, these data revealed that the *A. thaliana* plant can strongly use as a successfully transformation system for study the terpene synthase genes in *S. officinalis*.

Table 1. The major Terpenoid compositions in transgenic *A. thaliana* leave over-expressing of *SoFLDH*.

N	Compound name	R.T (min.)	Formula	Molecular Mass (g mol ⁻¹)	Terpene Type	% Peak area	
						AtW.T	SoFLDH
1	Dimethylsiloxane pentamer	19.503	C10H30O5Si5	370.7697			1.16
2	Thiourea, tetramethyl-	22.326	C5H12N2S	132.227		1.41	-
3	Dodecamethylcyclohexasiloxane	26.276	C12H36O6Si6	444.9236		-	2.32
4	Levo- β -Elemene	29.297	C15H24	204.3511	Sesqui	-	1.9
5	Cis-Caryophyllene	30.303	C15H24	204.3511	Sesqui	-	1.54
6	Tetradecamethylcycloheptasiloxane	31.896	C14H42O7Si7	519.0776		-	4.58
7	Gamma.-Muuroolene	32.328	C15H24	204.3511	Sesqui	-	9.04
8	Topanol O	33.006	C15H24O	220.3505		-	2.02
9	(-)- β -Bourbonene	35.301	C15H24	204.3511	Sesqui	-	2.2
10	Hexadecamethylcyclooctasiloxane	36.82	C16H48O8Si8	593.2315		-	2.9
11	Allethrin	38.032	C19H26O3	302.4079		-	1.33
12	Pyrethrin I	38.456	C21H28O3	328.4452		-	2.1
13	Cis-Thujanol	39.599	C10H18O	154.2493	Mono	-	0.89
14	Octadecamethylcyclononasiloxane	41.04	C18H54O9Si9	667.3855		-	2.23
15	Phytan	41.196	C20H42	282.5475	Diter	2.76	-
16	Hexahydrofarnesyl acetone	42.676	C18H36O	268.4778		-	1.95
17	Oleic Acid	43.799	C18H34O2	282.468		3.00	-
18	Cyclohexasiloxane, dodecamethyl-	44.792	C12H36O6Si6	444.9236		-	1.31
19	Palmitic acid	45.31	C16H32O2	256.4241		31.16	-
20	(Z)-9-Tetradecenal	46.587	C14H26O	210.3556		-	1.41
21	Palmitic acid, trimethylsilyl ester	47.316	C19H40O2Si	328.6052		5.69	-
22	Methyl dehydroabietate	47.469	C21H30O2	314.4617		-	2.49
23	Heneicosane	48.625	C21H44	296.5741		3.73	-
24	Trans-Phytol	49.213	C20H40O	296.531	Diter	-	30.49
25	Trans-Elaidic acid	49.488	C18H34O2	282.4614		29.59	-
26	Dodecanoyl chloride	49.889	C12H23ClO	218.763		-	10.35
27	Heptadecane, 8-methyl-	50.911	C17H36	240.4677		1.84	-
28	Octadecamethylcyclononasiloxane	51.454	C18H54O9Si9	667.3855		-	1.12
29	Cadinane	51.916	C20H41Cl	316.993	Diter	10.36	-
30	4-Methyldodecane	54.362	C13H28	184.3614		-	1.11
31	Stigmasterol acetate	57.289	C31H50O2	454.7275		-	1.05
32	Octadecamethylcyclononasiloxane	61.974	C18H54O9Si9	667.3855		-	0.77
33	Farnesan	63.242	C15H32	212.4146	Sesqui	-	0.78
34	Bis(2-ethylhexyl) phthalate	64.443	C24H38O4	390.5561		-	6.5
35	Dihomo- γ -linolenic acid; (Z,Z,Z)-icosatri-8,11,14-enoic acid	65.99	C20H34O2	306.4828		-	1.37
36	Heneicosane	74.674	C21H44	296.5741		-	3.97
37	2,6,10,14-Hexadecatetraen-1-ol, 3,7,11,15-tetramethyl-, acetate, (E,E,E)-	77.731	C22H36O2	332.5200		-	1.12
38	Tetrapentacontane	78.973	C54H110	759.4512		10.46	-
	Total % Peak area					% 100	% 100
	Total Percentage of Monoterpenes					-	0.89
	Total Percentage of Sesquiterpenes					-	15.46
	Total Percentage of Diterpenes					13.12	30.49

<https://doi.org/10.1371/journal.pone.0269045.t001>

Supporting information

S1 Fig. Typical GC-MS mass spectrographs for terpenoids from leaf of *A. thaliana* plants. (DOCX)

Acknowledgments

Our sincere appreciation for supporting of the Academy of Scientific Research and Technology (ASRT) with the National Natural Science Foundation of China and with the Egyptian Deserts Gene Bank, Desert Research Center. The authors thank Professor Dr. Osama Ezzat Elsayed and Dr. Aamir Hamid Khan for proof-reading the manuscript.

Author Contributions

Conceptualization: Mohammed Ali.

Formal analysis: Mohamed Hamdy Amar.

Methodology: Mohammed Ali, Elsayed Nishawy, Mohamed Ewas, Ahmed H. M. Hassan, Shengwei Wang.

Project administration: Guang-Wan Hu.

Resources: Mokhtar Said Rizk, Ahmed G. M. Sief-Eldein.

Supervision: Mohamed Hamdy Amar, Qing-Feng Wang.

Validation: Walaa A. Ramadan, Mokhtar Said Rizk, Mohamed Abd S. El-Zayat, Mingquan Guo, Fatma A. Ahmed.

Visualization: Elsayed Nishawy.

Writing – original draft: Mohammed Ali, Elsayed Nishawy, Shengwei Wang.

Writing – review & editing: Elsayed Nishawy, Mohamed Hamdy Amar, Qing-Feng Wang.

References

1. Alziar G. Catalogue synonymique des *Salvia* L. dumonde (Lamiaceae). I.–VI. Biocosme Mesogéen., 1988; 5:87–136.
2. Sarrou E, Ganopoulos I, Xanthopoulou A, et al. Genetic diversity and metabolic profile of *Salvia officinalis* populations: implications for advanced breeding strategies. *Planta*. 2017; 246(2):201–215. <https://doi.org/10.1007/s00425-017-2666-z> PMID: 28314999
3. Ali M, Li P, She G, Chen D, Wan X, Zhao J. Transcriptome and metabolite analyses reveal the complex metabolic genes involved in volatile terpenoid biosynthesis in garden sage (*Salvia officinalis*). *Scientific reports*. 2017; 7(1). <https://doi.org/10.1038/s41598-017-15478-3> PMID: 29167468
4. Ali M, Hussain RM, Rehman NU, et al. De novo transcriptome sequencing and metabolite profiling analyses reveal the complex metabolic genes involved in the terpenoid biosynthesis in Blue Anise Sage (*Salvia guaranitica* L.). *DNA Research*. 2018; 25(6):597–617. <https://doi.org/10.1093/dnares/dsy028> PMID: 30188980
5. Takano A, Okada H. Phylogenetic relationships among subgenera, species, and varieties of Japanese *Salvia* L. (Lamiaceae). *Journal of plant research*. 2011; 124(2):245–252. <https://doi.org/10.1007/s10265-010-0367-9> PMID: 20628783
6. Li D, Shao F, Lu S. Identification and characterization of mRNA-like noncoding RNAs in *Salvia miltiorrhiza*. *Planta*. 2015; 241(5):1131–1143. <https://doi.org/10.1007/s00425-015-2246-z> PMID: 25601000
7. Wang B, Sun W, Li Q, et al. Genome-wide identification of phenolic acid biosynthetic genes in *Salvia miltiorrhiza*. *Planta*. 2015; 241(3):711–725. <https://doi.org/10.1007/s00425-014-2212-1> PMID: 25471478

8. Bai Z, Li W, Jia Y, et al. The ethylene response factor SmERF6 co-regulates the transcription of SmCPS1 and SmKSL1 and is involved in tanshinone biosynthesis in *Salvia miltiorrhiza* hairy roots. *Planta*. 2018; 248(1):243–255. <https://doi.org/10.1007/s00425-018-2884-z> PMID: 29704055
9. Bohlmann J, Meyer-Gauen G, Croteau R. Plant terpenoid synthases: molecular biology and phylogenetic analysis. *Proceedings of the National Academy of Sciences, Biochemistry*. 1998; 95(8):4126–4133. <https://doi.org/10.1073/pnas.95.8.4126> PMID: 9539701
10. Xi J, Rossi L, Lin X, Xie DY. Overexpression of a synthetic insect-plant geranyl pyrophosphate synthase gene in *Camelina sativa* alters plant growth and terpene biosynthesis. *Planta*. 2016; 244(1):215–230. <https://doi.org/10.1007/s00425-016-2504-8> PMID: 27023458
11. Abbas F, Ke Y, Yu R, Fan Y. Functional characterization and expression analysis of two terpene synthases involved in floral scent formation in *Lilium* 'Siberia'. *Planta*. 2019; 249(1):71–93. <https://doi.org/10.1007/s00425-018-3006-7> PMID: 30218384
12. Wallach O. Zur Kenntniss der Terpene und der therischen Oele; F nfte Abhandlung. *Justus Liebigs Annalen der Chemie*. 1886; 239(1): 1–54.
13. Ruzicka L. The isoprene rule and the biogenesis of terpenic compounds. *Experientia*. 1953; 9(10): 357–367. <https://doi.org/10.1007/BF02167631> PMID: 13116962
14. Ruzicka L. Faraday Lecture (History of the isoprene rule). *Proceedings of the Chemical Society of London*, (11).1959; 341–360.
15. Ruzicka L. In the borderland between bioorganic chemistry and biochemistry. *Annual review of biochemistry*. 1973; 42: 1–21. <https://doi.org/10.1146/annurev.bi.42.070173.000245> PMID: 4600996
16. Trapp S, Croteau R. Defensive Resin Biosynthesis in Conifers. *Annual review of plant biology*. 2001; 52(1):689–724. <https://doi.org/10.1146/annurev.arplant.52.1.689> PMID: 11337413
17. Gershenzon J, Kreish W. Biochemistry of terpenoids: monoterpenes, sesquiterpenes, diterpenes, sterols, cardiac glycosides and steroid saponins. *Biochemistry of plant secondary metabolism*. 1999; (2): 222–299.
18. Tholl D, Boland W, Hansel A, Loreto F, Röse US, Schnitzler JP. Practical approaches to plant volatile analysis. *The Plant Journal*.2006; 45 (4):540–560. <https://doi.org/10.1111/j.1365-313X.2005.02612.x> PMID: 16441348
19. Aziz R A, Hamed F K, Abdulah N A. Determination of the main components of the essential oil extracted from *Salvia fruticosa* by sing GC and GC-MS DAMASCUS. *Journal of Agriculture Science*. 2008; 24:223–236.
20. Loizzo M R, Menichini F, Tundis R, et al. Comparative chemical composition and antiproliferative activity of aerial parts of *Salvia leriifolia* Benth and *Salvia acetabulosa* L. essential oils against human tumor cell *in vitro* models. *Journal of Medicinal Food*. 2010; 13(1):62–69. <https://doi.org/10.1089/jmf.2009.0060> PMID: 20136437
21. Takano A, Okada H. Phylogenetic relationships among subgenera, species, and varieties of Japanese *Salvia* L. (Lamiaceae). *Journal plant research*. 2011; 124(2):245–252. <https://doi.org/10.1007/s10265-010-0367-9> PMID: 20628783
22. Wenping H, Yuan Z, Jie S, Lijun Z, Zhezhi W. De novo transcriptome sequencing in *Salvia miltiorrhiza* to identify genes involved in the biosynthesis of active ingredients. *Genomics*. 2011; 98(4):272–279. <https://doi.org/10.1016/j.ygeno.2011.03.012> PMID: 21473906
23. Nadaf M, Nasrabadi M, Halimi M. GC-MS analysis of n-hexane extract from aerial parts of *Salvia nemorosa*. *Middle-East Journal of Scientific Research*. 2012; 11(8): 1127–1130.
24. Fateme A M, Mohammad H F, Abdolhossein R, Ali Z, Maryam S. Volatile Constituents of *Salvia compressa* and *Logochilus macranthus*, two Labiatae Herbs Growing wild in Iran. *Research Journal of Recent Sciences*. 2013; 2(2): 66–68.
25. Ahmad-Sohdi NA, Seman-Kamarulzaman AF, Mohamed-Hussein ZA, Hassan M. Purification and Characterization of a Novel NAD(P)⁺-Farnesol Dehydrogenase from *Polygonum minus* Leaves. *PLoS One*. 2015; 10 (11): e0143310. <https://doi.org/10.1371/journal.pone.0143310> PMID: 26600471
26. Ali M, Miao L, Hou Q, Darwish DB, Alrdahe SS, Ali A, et al. Overexpression of Terpenoid Biosynthesis Genes from Garden Sage (*Salvia officinalis*) Modulates Rhizobia Interaction and Nodulation in Soybean. *Front Plant Sci*. 2021; 12, 783269. <https://doi.org/10.3389/fpls.2021.783269> PMID: 35003167
27. Hussain RM, Ali M, Feng X, and Li X. The essence of NAC gene family to the cultivation of drought-resistant soybean (*Glycine max* L. Merr.) cultivars. *BMC Plant Biol*. 2017; 17(1):55. <https://doi.org/10.1186/s12870-017-1001-y> PMID: 28241800
28. Ma Z, Cooper C, Kim HJ, Janick-Buckner D. A study of rubisco through western blotting and tissue printing techniques. *CBE Life Sci Educ*. 2009; Summer; 8(2):140–6. <https://doi.org/10.1187/cbe.09-01-0003> PMID: 19487503.

29. Aharoni A, Giri AP, Deuerlein S, et al. Terpenoid metabolism in wild-type and transgenic Arabidopsis plants. *The Plant Cell*. 2003; 15(12):2866–2884. <https://doi.org/10.1105/tpc.016253> PMID: 14630967
30. Ee SF, Mohamed-Hussein ZA, Othman R, Shaharuddin NA, Ismail I, Zainal Z. Functional characterization of sesquiterpene synthase from *Polygonum minus*. *The Scientific World Journal*. 2014; <https://doi.org/10.1155/2014/840592> PMID: 24678279
31. Mehmood N, Yuan Y, Ali M, et al. Early transcriptional response of terpenoid metabolism to *Colletotrichum gloeosporioides* in a resistant wild strawberry *Fragaria nilgerrensis*. *Phytochemistry*. 2021; 181:112590. <https://doi.org/10.1016/j.phytochem.2020.112590> PMID: 33232864
32. Rebecca S W, Ayelign MA, Lina B, Elaheh N, Soheil SM. Cloning and functional characterization of a floral repressor gene from *Lavandula angustifolia*. *Planta*. 2020; 251(41):1–11. <https://doi.org/10.1007/s00425-019-03333-w> PMID: 31907678
33. Whittington DA, Wise ML, Urbansky M, Coates RM, Croteau RB, Christianson DW. Bornyl diphosphate synthase: structure and strategy for carbocation manipulation by a terpenoid cyclase. *Proceedings of the National Academy of Science*. 2002; 99(24):15375–15380. <https://doi.org/10.1073/pnas.232591099> PMID: 12432096
34. Hyatt DC, Youn B, Zhao Y, et al. Structure of limonene synthase, a simple model for terpenoid cyclase catalysis. *Proceedings of the National Academy of Science*. 2007; 104(13):5360–5365. <https://doi.org/10.1073/pnas.0700915104> PMID: 17372193
35. Oppermann UC, Filling C, Berndt KD, Persson B, Benach J, Ladenstein R, et al. Active site directed mutagenesis of $3\beta/17\beta$ -hydroxysteroid dehydrogenase establishes differential effects on short-chain dehydrogenase/reductase reactions. *Biochemistry*. 1997; 36(1): 34–40. <https://doi.org/10.1021/bi961803v> PMID: 8993315
36. Ziegler J, Voigtländer S, Schmidt J, et al. Comparative transcript and alkaloid profiling in *Papaver* species identifies a short chain dehydrogenase/reductase involved in morphine biosynthesis. *The Plant Journal*. 2006; 48(2):177–192. <https://doi.org/10.1111/j.1365-313X.2006.02860.x> PMID: 16968522
37. Geissler R, Brandt W, Ziegler J. Molecular modeling and site-directed mutagenesis reveal the benzylisoquinoline binding site of the short-chain dehydrogenase/reductase salutaridine reductase. *Plant physiology*. 2007; 143 (4):1493–1503. <https://doi.org/10.1104/pp.106.095166> PMID: 17337529
38. Su-Fang E, Zeti-Azura M, Roohaida O, Noor AS, Ismanizan I, and Zamri Z. Functional Characterization of Sesquiterpene Synthase from *Polygonum minus*. *ScientificWorldJournal*. 2014; <https://doi.org/10.1155/2014/840592> PMID: 24678279
39. Degenhardt J, Köllner TG, and Gershenzon J. Monoterpene and sesquiterpene synthases and the origin of terpene skeletal diversity in plants. *Phytochemistry*, 2009; 70(15–16), 1621–1637. <https://doi.org/10.1016/j.phytochem.2009.07.030> PMID: 19793600
40. Zhao L, Zhao X, Francis F, and Liu Y. Genome-wide identification and characterization of the TPS gene family in wheat (*Triticum aestivum* L.) and expression analysis in response to aphid damage. *Acta Physiol Plant*. 2021; 43, 64. <https://doi.org/10.1007/s11738-021-03236-y>
41. Liu J, Huang F, Wang X, Zhang M, Zheng R, Wang J, et al. Genome-wide analysis of terpene synthases in soybean: functional characterization of *GmTPS3*. *Gene*. 2014; 544(1), 83–92. <https://doi.org/10.1016/j.gene.2014.04.046> PMID: 24768723
42. Taniguchi S, Miyoshi S, Tamaoki D, Yamada S, Tanaka K, Uji Y, et al. Isolation of jasmonate-induced sesquiterpene synthase of rice: product of which has an antifungal activity against *Magnaporthe oryzae*. *J. Plant Physiol*. 2014; 171, 625–632. <https://doi.org/10.1016/j.jplph.2014.01.007> PMID: 24709155
43. Chen X, Chen H, Yuan JS, Köllner TG, Chen Y, Guo Y, et al. The rice terpene synthase gene *OsTPS19* functions as an (S)-limonene synthase in planta, and its overexpression leads to enhanced resistance to the blast fungus *Magnaporthe oryzae*. *Plant Biotechnol J*. 2018; 16(10):1778–1787. <https://doi.org/10.1111/pbi.12914> PMID: 29509987
44. Wang Y, Yang Q, Zhu Y, Zhao L, Ju P, Wang G, et al. MrTPS3 and MrTPS20 Are Responsible for β -Caryophyllene and α -Pinene Production, Respectively, in Red Bayberry (*Morella rubra*). *Front Plant Sci*. 2022; 12, 798086. <https://doi.org/10.3389/fpls.2021.798086> PMID: 35069655
45. Marmont LS, Whitfield GB, Pfoh R, et al. PelX is a UDP-N-acetylglucosamine C4-epimerase involved in Pel polysaccharide-dependent biofilm formation. *Journal of Biological Chemistry*. 2020; 295 (34):11949–11962. <https://doi.org/10.1074/jbc.RA120.014555> PMID: 32601062
46. Shimada T, Endo T, Fujii H, Hara M, Omura M. Isolation and characterization of (E)-beta-ocimene and 1,8 cineole synthases in *Citrus unshiu* Marc. *Plant Science*. 2005; 168(4):987–995.
47. Lückner J, El Tamer MK, Schwab W, et al. Monoterpene biosynthesis in lemon (*Citrus limon*). cDNA isolation and functional analysis of four monoterpene synthases. *European Journal of Biochemistry*. 2002; 269(13):3160–3171. <https://doi.org/10.1046/j.1432-1033.2002.02985.x> PMID: 12084056

48. Fahrnich A, Krause K, Piechulla B. Product variability of the 'cineole cassette' monoterpene synthases of related *Nicotiana* species. *Molecular Plant*. 2011; 4(6):965–984. <https://doi.org/10.1093/mp/ssr021> PMID: 21527560
49. Faldt J, Martin D, Miller B, Rawat S, Bohlmann J. Traumatic resin defense in Norway spruce (*Picea abies*): methyl jasmonate-induced terpene synthase gene expression, and cDNA cloning and functional characterization of (+)-3-carene synthase. *Plant Molecular Biology*. 2003; 51(1):119–133. <https://doi.org/10.1023/a:1020714403780> PMID: 12602896